Transverse acoustic waves in piezoelectric and ferroelectric antiphase superlattices

A. L. Shuvalov* and A. S. Gorkunova
Institute of Crystallography, Russian Academy of Sciences, Leninsky prospect 59, Moscow 117333, Russia
(Received 5 October 1998)

The diffraction of a shear horizontally polarized acoustic wave is analyzed at an oblique incidence upon the superlattice, which describes a system of 180° ferroelectric domains or a stack of antiparallel piezoelectric layers. The formalism of 4×4 propagator-matrix formalism, which takes into account the electromechanical coupling, is pursued. The developed algebraic procedure provides a comprehensive analytical description of the reflection and transmission rates in an explicit and concise form. This allows direct examination of the resonant features of the reflection and transmission spectra at an unrestricted variation of the involved parameters. In the case of nonequidistant superlattices, the modulation of the Bragg peaks is characterized and the extinction rule deduced. [S0163-1829(99)08113-8]

I. INTRODUCTION

Elastodynamics of multilayered media has been attracting steady interest in recent years with respect to both the acoustic-phonon properties of nanometer superlattices and the elastic-wave diffraction phenomena.[1–18] A large number of materials utilized for fabricating nanometer superlattices have piezoelectric properties. In parallel, a ''natural'' diffraction grate is provided by regular structures of 180° ferroelectric domains, which are created by means of a certain crystal-growth treatment or by applying the electric bias of alternating sign to a monocrystal in the process of the ferroelectric phase transition. The manufacturing technique for various ferroelectric crystals delivers good-quality periodic structures with a single-domain width in the range 5–300 μm (thickness of domain walls is typically of the order $10^{-1}-10^{-2}$ μm). The acoustic and optical properties of such ferroelectric superlattices have been the object of many experimental and theoretical studies (e.g., see Refs. 6,8,9,11,13,15).

One of the most effective theoretical tools for the exact analytical study of various wave phenomena in periodically stratified media is the method of the propagator matrix based on the Bloch formalism. However, the direct analytical calculations become very cumbersome once the dimension of the propagator matrix is higher than 2×2 due to the coupled-mode effect. It occurs, for instance, at a mixing of the sagittal acoustic modes in a symmetry plane of purely elastic stratified media,[1,2,4,14,17] or at the *SH* waves propagation in the presence of electromechanical coupling.[2,3,5,8,12,16] As a result, theoretical treatment in those cases is largely numerical. The explicit analytical results have been mainly confined to obtaining the Bloch dispersion relation (the characteristic equation for the propagator matrix), whereas the direct analytical calculation of the reflection rate itself has been discussed under certain fairly restrictive approximations and assumptions. In particular, in Refs. 12 and 16 the propagator matrix has been effectively reduced to the 2×2 dimension thanks to the screening properties of metallized interfaces separating piezoelectric layers. The calculation of the reflection coefficient was then carried out under the condition $q^2 \tan\theta \ll 1$, where θ is the angle of incidence and q^2 is the parameter of electromechanical coupling. The analytical method, which has been worked out in Ref. 17, assumes a semi-infinite periodic structure and a normal incidence in the case of solid layers. The reflection coefficient[17] was obtained in a somewhat implicit form, via the root of a matrix equation.

This paper is concerned with the oblique propagation of the *SH* wave in a regular structure of 180° ferroelectric domains, which are characterized by the same elastic properties and pairwise differ in the sign of their piezoelectric coefficients. This antiphase superlattice may also describe a system of piezoelectric layers of the same material, which are stacked in such a way that the orientations of the principal symmetry axes in neighboring layers are antiparallel. (For definiteness, we will thereafter refer to the case of ferroelectric domains.) Due to electromechanical coupling at elastic-wave propagation, alternation of signs of the piezoelectric coefficients stipulate the excitation of the interface modes of the electric field and the reflection of the *SH* wave at the interfaces. Invoking the formalism of a propagator matrix, which herein is of the 4×4 dimension, we pursue the algebraic procedure and obtain the explicit expressions, that comprehensively characterize the spectral dependence of the reflection rate. The only approximation used is based on the strong inequality $\exp[-2\pi(d/\lambda)\sin\theta]\ll 1$, where d is the domain width, λ is the wavelength ($\theta=0$ corresponds to the normal incidence, at which the *SH* mode uncouples from electric field and becomes nonpiezoactive). Exponential accuracy of this approximation ensures its virtual exactness for describing the Bragg-resonance features of diffraction.

II. BACKGROUND

Propagation of plane acoustic waves in a medium with piezoelectric properties is governed by the equations

$$\sigma_{ij,j}=\rho\ddot{u}_i, \quad D_{i,i}=0;$$

$$\sigma_{ij}=c_{ijkl}u_{k,l}+e_{kij}\varphi_{,k}, \quad D_i=-\varepsilon_{ij}\varphi_{,j}+e_{ijk}u_{j,k}, \quad (1)$$

where the comma in the subscripts and superposed dot imply spatial and time derivatives, respectively; ρ is the density, σ_{jk} is the tensor of mechanical stress, $\mathbf{u}$ is the vector of

 ©1999 The American Physical Society

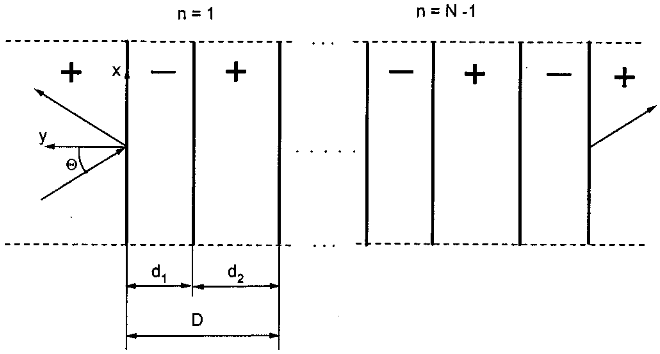

FIG. 1. An antiphase superlattice.

elastic displacement, **D** is the vector of electric induction, φ is the electric potential. We consider the periodic structure of 180° domains in a ferroelectric crystal of the $4mm$ symmetry class ($BaTiO_3$ or $PbTiO_3$ are typical examples). The vector of spontaneous polarization is directed along the principal symmetry axis and has antiparallel orientations in the neighboring domains. It lies in the plane of domain walls which coincides with a symmetry plane. Let the axis Y be orthogonal to the interfaces, and the axis Z be parallel to the fourfold axis (Fig. 1). The mutual orientation of symmetry elements in adjoined 180° domains are related by the center of inversion, which pertained to the paraelectric phase of the crystal. Hence, both types of domains are characterized by the same even-rank tensors of elastic moduli c_{ijkl} and dielectric permittivity ε_{ij}, while components of the odd-rank tensor of piezoelectricity e_{ijk} have opposite signs in neighboring domains constituting a unit cell. Its width $D=d_1+d_2$ is the period of the superlattice ($D=2d$ in the case of an equidistant structure). The system of $2N-1$ domains is supposed to be bounded from both sides by the monodomain (homogeneous) substrates of the same ferroelectric crystal. Taking the piezoelectric coefficients e_{ijk} of the substrates as reference ones assigns the values $-e_{ijk}$ and e_{ijk} to, respectively, the first and the second domain of each unit cell (domains of "$-$" and "$+$" types).

Suppose that the *SH* wave, propagating in the plane *XY* and polarized along the axis *Z* (Fig. 1), falls upon the domain superlattice at the angle of incidence θ ($\theta\neq 0$). According to Eqs. (1), this mode is uncoupled from the two other elastic modes, but at the same time it couples with quasistatic electric field. Due to opposite signs of piezoelectric coefficients in neighboring domains, a single *SH* acoustoelectric wave does not fulfill the continuity of the displacement u_z, traction $f_z=-ik_x\sigma_{32}$, potential φ, and the normal component of electric induction D_y. This results in reflection at interfaces, which is specular for symmetry reasons, and in excitation of two interface modes. On appealing to Eqs. (1), the aforementioned wave parameters in a given domain of nth cell may be presented in the form

$$\begin{pmatrix} u_z(y) \\ \varphi(y) \\ ik_x^{-1}f_z(y) \\ ik_x^{-1}D_y(y) \end{pmatrix}^{(n,\mp)} = b_i^{(n,\mp)} \begin{pmatrix} 1 \\ \mp e_{15}/\varepsilon_{11} \\ c'_{44}\cot\theta \\ 0 \end{pmatrix} e^{-ik_y(y+nD)} + b_r^{(n,\mp)} \begin{pmatrix} 1 \\ \mp e_{15}/\varepsilon_{11} \\ -c'_{44}\cot\theta \\ 0 \end{pmatrix} e^{ik_y(y+nD)}$$

$$+ b_s^{(n,\mp)} \begin{pmatrix} 0 \\ 1 \\ \pm ie_{15} \\ i\varepsilon_{11} \end{pmatrix} e^{-k_x(y+nD)} + b_{s'}^{(n,\mp)} \begin{pmatrix} 0 \\ 1 \\ \mp ie_{15} \\ -i\varepsilon_{11} \end{pmatrix} e^{k_x(y+nD)} \qquad (2)$$

(the common factor $\exp[i(k_x x-\omega t)]$ is suppressed). In Eq. (2), the notations used are $c'_{44}=c_{44}+(e_{15}^2/\varepsilon_{11})$, $k_x=k\sin\theta$, $k_y=k\cos\theta$, $k=\omega(c'_{44}/\rho)^{-1/2}$; the upper and lower signs correspond to the domains of, respectively, "$-$" and "$+$" types; and the subscripts i,r,s,s' are assigned to the partial amplitudes of, respectively, the incident, reflected, and two interface modes. Invoking the boundary conditions of continuity at interfaces $y=-(n-1)D$ and $y=-(n-1)D-d_1$ (Fig. 1), then eliminating the four-component vector $\mathbf{b}^{(n,-)}$ of partial amplitudes $b_i^{(n,-)}$, $b_r^{(n,-)}$, $b_s^{(n,-)}$, $b_{s'}^{(n,-)}$ in the standard fashion, yields the relation

$$\mathbf{b}^{(n-1,+)}=\mathbf{W}\mathbf{b}^{(n,+)}. \qquad (3)$$

Here the 4×4 propagator matrix **W**, transferring the column of partial amplitudes through a unit cell, has the form

$$\mathbf{W}=\begin{pmatrix} e^{-ik_yD}-2iq_\theta^2 e^{-ik_yd_2}\sinh(k_xd_1) & -2iq_\theta^2 e^{ik_yd_2}\sinh(k_xd_1) & -i\dfrac{e_{15}\tan\theta}{c_{44}}e^{-k_xD}(1-e^{k_xd_1-ik_yd_1}) & i\dfrac{e_{15}\tan\theta}{c_{44}}e^{k_xD}(1-e^{-k_xd_1-ik_yd_1}) \\ 2iq_\theta^2 e^{-ik_yd_2}\sinh(k_xd_1) & e^{ik_yD}+2iq_\theta^2 e^{ik_yd_2}\sinh(k_xd_1) & i\dfrac{e_{15}\tan\theta}{c_{44}}e^{-k_xD}(1-e^{k_xd_1+ik_yd_1}) & -i\dfrac{e_{15}\tan\theta}{c_{44}}e^{k_xD}(1-e^{-k_xd_1+ik_yd_1}) \\ \dfrac{e_{15}}{\varepsilon_{11}}e^{-ik_yD}(1-e^{-k_xd_1+ik_yd_1}) & \dfrac{e_{15}}{\varepsilon_{11}}e^{ik_yD}(1-e^{-k_xd_1-ik_yd_1}) & e^{-k_xD}+2q_\theta^2 e^{-k_xd_2}\sin(k_yd_1) & -2q_\theta^2 e^{k_xd_2}\sin(k_yd_1) \\ \dfrac{e_{15}}{\varepsilon_{11}}e^{-ik_yD}(1-e^{k_xd_1+ik_yd_1}) & \dfrac{e_{15}}{\varepsilon_{11}}e^{ik_yD}(1-e^{k_xd_1-ik_yd_1}) & 2q_\theta^2 e^{-k_xd_2}\sin(k_yd_1) & e^{k_xD}-2q_\theta^2 e^{k_xd_2}\sin(k_yd_1) \end{pmatrix}, \qquad (4)$$

in which

$$q_\theta^2 = q^2 \tan\theta, \quad q^2 = \frac{e_{15}^2}{c'_{44}\varepsilon_{11}}, \tag{5}$$

q^2 is the parameter of electromechanical coupling. Thereupon, the partial amplitudes of the wave fields at the entrance and at the exit of the superlattice are related as follows:

$$\begin{pmatrix} b_i \\ b_r \\ b_s \\ 0 \end{pmatrix}^{(\mathrm{en})} = \mathbf{W}^N \begin{pmatrix} b_i \\ 0 \\ 0 \\ b_{s'} \end{pmatrix}^{(\mathrm{ex})}, \tag{6}$$

where $b_i^{(\mathrm{en})}$, $b_r^{(\mathrm{en})}$ are the amplitudes of, respectively, the incident and reflected *SH* waves at the front face of the superlattice; $b_i^{(\mathrm{ex})} \equiv b_t$ is the amplitude of the *SH* wave transmitted through the superlattice; $b_s^{(\mathrm{en})}$ and $b_{s'}^{(\mathrm{en})}$ are the amplitudes of the evanescent interfacial waves decreasing away from the entrance and exit interfaces, respectively. Eliminating the amplitudes, referred to the exit, delivers the reflection coefficient $R \equiv b_r^{(\mathrm{en})}/b_i^{(\mathrm{en})}$ in terms of the propagator matrix:

$$R = \frac{(\mathbf{W}^N)_{21}(\mathbf{W}^N)_{44} - (\mathbf{W}^N)_{24}(\mathbf{W}^N)_{41}}{(\mathbf{W}^N)_{11}(\mathbf{W}^N)_{44} - (\mathbf{W}^N)_{14}(\mathbf{W}^N)_{41}}. \tag{7}$$

The Nth power of the matrix $\mathbf{W}$ with the nondegenerate eigenvalues λ_α ($\alpha = 1,\ldots,4$) may be defined by the relation[19]

$$(\mathbf{W}^N)_{ik} = \sum_{\alpha=1}^{4} \lambda_\alpha^N \Omega_{i\alpha} (\Omega^{-1})_{\alpha k} = \frac{1}{\det\|\Omega\|} \sum_{\alpha=1}^{4} \lambda_\alpha^N \Omega_{i\alpha} \overline{\Omega}_{\alpha k}, \tag{8}$$

where $\|\Omega\| = \Omega_{i\alpha}$ ($i,\alpha = 1,\ldots,4$) is the matrix constituted by the components of the eigenvectors $\mathbf{\Omega}_\alpha$ of $\mathbf{W}$ [note that they may figure in Eq. (8) bearing arbitrary normalization], and $\overline{\Omega}_{\alpha k}$ are components of the adjugate matrix $\overline{\|\Omega\|}$.

III. ALGEBRAIC FORMALISM

A. General relations for the eigenvalues and eigenvectors of the propagator matrix

In accordance with the general theory of the Bloch formalism,[20] the propagator matrix $\mathbf{W}$ (4) is unimodular ($\det \mathbf{W} = 1$) due to the symmetry of the considered problem, and its eigenvalues λ_α may be presented in the form

$$\lambda_\alpha = e^{iK_\alpha D}, \quad \alpha = 1,2,3,4,$$
$$\lambda_1 = 1/\lambda_2, \quad \lambda_3 = 1/\lambda_4, \tag{9}$$

where K_α ($K_1 = -K_2, K_3 = -K_4$) are termed the Bloch wave numbers. The characteristic polynomial of a 4×4 matrix $\mathbf{W}$ is[19]

$$\det(\mathbf{W} - \lambda\mathbf{I}) = \prod_{\alpha=1}^{4} (\lambda_\alpha - \lambda) = \lambda^4 - p_1\lambda^3 - p_2\lambda^2 - p_3\lambda - p_4, \tag{10}$$

where

$$p_1 = \mathrm{tr}\,\mathbf{W}, \quad p_2 = \frac{1}{2}[\mathrm{tr}(\mathbf{W}^2) - (\mathrm{tr}\,\mathbf{W})^2],$$

$$p_3 = \frac{1}{3}\mathrm{tr}(\mathbf{W}^3) - \frac{1}{2}(\mathrm{tr}\,\mathbf{W}^2)(\mathrm{tr}\,\mathbf{W}) + (\mathrm{tr}\,\mathbf{W})^3, \quad p_4 = -\det\mathbf{W}, \tag{11}$$

tr denotes the trace of a matrix, $\mathbf{I}$ is the 4×4 identity matrix. Using Eq. (9), one may cast Eq. (10) into the form

$$\det(\mathbf{W} - \lambda\mathbf{I}) = \lambda^4 - (\lambda_1 + \lambda_2 + \lambda_3 + \lambda_4)\lambda^3 + [(\lambda_1 + \lambda_2) \times (\lambda_3 + \lambda_4) + 2]\lambda^2 - (\lambda_1 + \lambda_2 + \lambda_3 + \lambda_4)\lambda + 1, \tag{12}$$

so that

$$p_1 = p_3 = \lambda_1 + \lambda_2 + \lambda_3 + \lambda_4, \quad p_2 = -(\lambda_1 + \lambda_2)(\lambda_3 + \lambda_4) - 2. \tag{13}$$

Equation (12) reveals that, thanks to Eq. (9), the fourth-order characteristic equation $\det(\mathbf{W} - \lambda\mathbf{I}) = 0$ is a reciprocal one (i.e., $p_1 = p_3$). Therefore, it may be reduced to a quadratic equation[5] (without actually calculating the matrix $\mathbf{W} + \mathbf{W}^{-1}$, as implemented in Ref. 2). Introducing

$$\mu_1 = \lambda_1 + \frac{1}{\lambda_1}, \quad \mu_3 = \lambda_3 + \frac{1}{\lambda_3}, \tag{14}$$

and appealing to Eqs. (9), (11), (13) readily yields

$$\mu_1 + \mu_3 = \mathrm{tr}\,\mathbf{W}, \quad \mu_1\mu_3 = \frac{1}{2}[(\mathrm{tr}\,\mathbf{W})^2 - \mathrm{tr}\,\mathbf{W}^2 - 4]. \tag{15}$$

Hence, by the Bezout theorem, one arrives at the characteristic equation in the form

$$\mu^2 - (\mathrm{tr}\,\mathbf{W})\mu + \frac{1}{2}[(\mathrm{tr}\,\mathbf{W})^2 - \mathrm{tr}\,\mathbf{W}^2 - 4] = 0. \tag{16}$$

which is equivalent to the presentations given in Refs. 5,2. Once Eq. (16) is solved, the eigenvalues λ_α ($\alpha = 1,\ldots,4$) may be found from the quadratic equations furnished by Eq. (14).

Next, we calculate the eigenvectors of the propagator matrix $\mathbf{W}$. Provided that the eigenvalues of $\mathbf{W}$ are nondegenerate, the components $\Omega_{i\alpha}$ of its eigenvectors $\mathbf{\Omega}_\alpha$ are given by the relation

$$\Omega_{i\alpha} = (\overline{\mathbf{W} - \lambda_\alpha\mathbf{I}})_{iq}, \quad i,\alpha = 1,2,3,4, \tag{17}$$

where the number q of the column of the adjugate matrix $\overline{\mathbf{W} - \lambda_\alpha\mathbf{I}}$ may be chosen arbitrarily, and correspondingly the normalization for the vectors $\mathbf{\Omega}_\alpha$ is not specified. The matrix $\overline{\mathbf{W} - \lambda\mathbf{I}}$ satisfies the identity[19]

$$\overline{\mathbf{W} - \lambda\mathbf{I}} = \lambda^3\mathbf{I} + \lambda^2\mathbf{W}^{(1)} + \lambda\mathbf{W}^{(2)} + \mathbf{W}^{(3)}, \tag{18}$$

in which

$$\mathbf{W}^{(1)} = \mathbf{W} - p_1\mathbf{I}, \quad \mathbf{W}^{(2)} = \mathbf{W}^2 - p_1\mathbf{W} - p_2\mathbf{I},$$
$$\mathbf{W}^{(3)} = \mathbf{W}^3 - p_1\mathbf{W}^2 - p_2\mathbf{W} - p_3\mathbf{I}, \tag{19}$$

where the coefficients p_1, p_2, p_3 are defined by Eq. (11) and obey relations (13). On multiplying $\mathbf{W}^{(3)}$ by $\mathbf{W}$, comparing the result with the characteristic polynomial (10), and then making use of the Cayley-Hamilton theorem, we find that $\mathbf{W}^{(3)}\mathbf{W}=p_4=-\det \mathbf{W}$, hence

$$\mathbf{W}^{(3)}=-\overline{\mathbf{W}}. \tag{20}$$

Inserting Eqs. (18)–(20) into Eq. (17) and invoking Eq. (9) delivers the following representation for the components of the eigenvectors $\mathbf{\Omega}_\alpha$ of $\mathbf{W}$:

$$\Omega_{i\alpha}=(\lambda_\alpha+\lambda_\gamma+\lambda_\delta)\delta_{iq}-(1+\lambda_\alpha\lambda_\gamma+\lambda_\alpha\lambda_\delta)W_{iq} + \lambda_\alpha(\mathbf{W}^2)_{iq}-\overline{W}_{iq}, \tag{21}$$

where δ_{iq} is the Kronecker symbol; $i=1,...,4$; q is any fixed column's number; $\alpha=1,\ldots,4$, and the other indices β, γ, δ are supposed to match the ordering $\lambda_\alpha\lambda_\beta=1$, $\lambda_\gamma\lambda_\delta=1$.

We note that knowledge of eigenvectors $\mathbf{\Omega}_\alpha$ ($\alpha=1,\ldots,4$) of $\mathbf{W}$ readily yields the Bloch eigenmodes $\mathbf{U}\mathbf{\Omega}_\alpha$ [$\mathbf{U}$ is the 4×4 matrix constituted by components of the vectors featured in the right-hand side of Eq. (2)], which are the eigenvectors of the similar propagator matrix $\mathbf{UWU}^{-1}$ transferring the wave field Eq. (2) through a unit cell.

B. Derivation of the reflection coefficient

At this stage we set the assumption

$$e^{-k_x d_i}\ll 1 \quad (i=1,2). \tag{22}$$

Another strong inequality

$$q_\theta^2 e^{-k_x d_i}\sin(k_y d_j)\ll 1 \quad (i,j=1,2), \tag{23}$$

also underlying the foregoing derivations, is virtually encapsulated in Eq. (22) for commensurable domain widths and any angle of incidence, including a nearly grazing one ($\theta\to\pi/2$), for which Eq. (23) implies $q^2 e^{-kd_i}kd_j\ll 1$ [see Eq. (5); recall also that typical values q^2 are of the order 10^{-2}–10^{-1}].

Inserting Eq. (4) into the quadratic equation (16), we may write its roots $\mu_{1,3}=\cos(K_{1,3}D)$ in the leading approximation (in neglect of terms $\sim e^{-k_x d_i}$) as

$$\cos(K_1 D)=\cos(k_y D)-2q_\theta^2[\sin(k_y D) - q_\theta^2 \sin k_y d_1 \sin k_y d_2], \tag{24}$$

$$\cos(K_3 D)=\frac{1}{2}e^{k_x D}-q_\theta^2[e^{k_x d_2}\sin(k_y d_1)+e^{k_x d_1}\sin(k_y d_2)] + 2q_\theta^2[\sin k_y D-q_\theta^2\sin(k_y d_1)\sin(k_y d_2)]. \tag{25}$$

Hence follow the eigenvalues $\lambda_{1,2}=\exp(\pm iK_1 D)$ and $\lambda_{3,4}=\exp(\pm iK_3 D)$. The indices $\alpha=1,2$ are assigned to those Bloch eigenmodes, which stem from the incident and reflected bulk *SH* waves, and the indices $\alpha=3,4$ are associated with the interface waves. Relating $\alpha=3$ and $\alpha=4$ to the decreasing and increasing waves, respectively, we obtain

$$\lambda_3=e^{-k_x D}, \tag{26}$$

$$\lambda_4=e^{k_x D}-2q_\theta^2[e^{k_x d_2}\sin(k_y d_1)+e^{k_x d_1}\sin(k_y d_2)] + 4q_\theta^2[\sin k_y D-q_\theta^2\sin(k_y d_1)\sin(k_y d_2)]. \tag{27}$$

It is seen that, in view of Eq. (22), the eigenvalues λ_α satisfy the exponentially strong inequalities

$$\lambda_3\ll|\lambda_1|, \quad |\lambda_2|\ll\lambda_4, \tag{28}$$

which are essential for the foregoing derivation of the reflection coefficient R. [Note that the next-order terms, retained in Eq. (27), will play an essential role in the forthcoming derivations.]

The above-mentioned provisions enable us to find the reflection coefficient (7) with the aid of Eq. (8) confining to the leading terms $O(\lambda_4^{2N})+O(\lambda_{1,2}^N\lambda_4^N)$. It appears that the terms, proportional to $\lambda_4^{2N}\sim e^{2Nk_x d}$, exactly compensate each other in both the numerator and the denominator of the right-hand side of Eq. (7). [This is certainly not an incidental occasion, since otherwise it would mean that the reflection rate in the leading order of the short-wavelength approximation (22) is totally determined by the inhomogeneous interface modes and is not affected by incident and diffracted bulk modes which is senseless.] As a result, the principal part of the reflection coefficient may be cast into the form

$$R=\frac{\lambda_1^{2N}p_{21}P+\lambda_2^{2N}p_{22}}{\lambda_1^{2N}p_{11}P+\lambda_2^{2N}p_{12}}, \tag{29}$$

where

$$p_{j\alpha}=\Omega_{j\alpha}\Omega_{44}-\Omega_{j4}\Omega_{4\alpha} \quad (j,\alpha=1,2),$$

$$P=\frac{\overline{\Omega}_{11}\overline{\Omega}_{44}-\overline{\Omega}_{14}\overline{\Omega}_{41}}{\overline{\Omega}_{21}\overline{\Omega}_{44}-\overline{\Omega}_{24}\overline{\Omega}_{41}}. \tag{30}$$

In order to calculate $p_{j\alpha}$, we insert the components $\Omega_{j\alpha}$ of eigenvectors $\mathbf{\Omega}_\alpha$ from Eq. (21) and then invoke the explicit form (4) of the propagator matrix $\mathbf{W}$ and its eigenvalue λ_4 Eq. (27). Adhering to the leading order in $e^{k_x d_{1,2}}$ by virtue of Eqs. (22), (28), we find

$$p_{j\alpha}=-\lambda_4^2\{\lambda_\alpha[W_{j4}(\mathbf{W}^2)_{44}-W_{44}(\mathbf{W}^2)_{j4}]+(\mathbf{W}^2)_{j4}\}$$
$$=\mp C\{1-\lambda_\alpha[e^{\mp ik_y D}-2q_\theta^2(\sin(k_y D)+e^{\mp ik_y d_1}\sin(k_y d_2)+2q_\theta^2\sin(k_y d_1)\sin(k_y d_2))]\},$$
$$j,\alpha=1,2, \tag{31}$$

where $j=1,2$ correspond to the upper and lower signs, respectively, and the common factor C, which stems from the definition (21) of unnormalized eigenvectors, is indeed arbitrary. Deriving P is more tedious but straightforward. An αj component of the adjugate matrix $\overline{\|\Omega\|}$ may be presented in the form of the mixed vector product $\overline{\Omega}_{\alpha j}=(-1)^{(\alpha+j)}[\mathbf{\Omega}_\beta(j),\mathbf{\Omega}_\gamma(j),\mathbf{\Omega}_\delta(j)]$ of three-dimensional vectors, obtained by crossing out the jth components from $\mathbf{\Omega}_\beta$, $\mathbf{\Omega}_\gamma$, $\mathbf{\Omega}_\delta$. This observation allows us to cancel those terms, in which any two of the multiplied vectors are parallel. Also, retaining only principal terms in accordance with Eqs. (22), (28) substantially facilitates the derivation. As a result, it yields the relation

$$P=-\frac{\lambda_2[\lambda_4(m_1-\lambda_4 m_2)-\lambda_1 m_1]}{\lambda_1[\lambda_4(m_1-\lambda_4 m_2)-\lambda_2 m_1]}, \tag{32}$$

where $m_1=(\mathbf{W}^2)_{24}\overline{W}_{34}-(\mathbf{W}^2)_{34}\overline{W}_{24}$, $m_2=W_{24}\overline{W}_{34}-W_{34}\overline{W}_{24}$. Invoking Eqs. (4) and (27), we obtain

$$P=-\frac{\lambda_2\{e^{ik_yD}-\lambda_1-2q_\theta^2[\sin(k_yD)+e^{ik_yd_1}\sin(k_yd_2)-2q_\theta^2\sin(k_yd_1)\sin(k_yd_2)]\}}{\lambda_1\{e^{ik_yD}-\lambda_2-2q_\theta^2[\sin(k_yD)+e^{ik_yd_1}\sin(k_yd_2)-2q_\theta^2\sin(k_yd_1)\sin(k_yd_2)]\}}. \tag{33}$$

Eventually, on inserting Eqs. (31), (33) into Eq. (29), we arrive at the desired relation for the reflection coefficient

$$R=\frac{2iq_\theta^2 e^{ik_y(d_2-d_1)}[\cos(k_yd_1)-q_\theta^2\sin(k_yd_1)]\sin(NK_1D)}{\{e^{-ik_yd_2}(1-2iq_\theta^2)+2iq_\theta^4[\sin(k_yd_2)-e^{ik_yd_1}\sin(k_y(d_2-d_1))]\}\sin NK_1D-e^{ik_yd_1}\sin[(N-1)K_1D]}, \tag{34}$$

[the next-order term $O(e^{-k_xd})$ is neglected]. Using Eqs. (34) and (24), the absolute value of the reflection rate squared is

$$|R|^2=\frac{Q^2}{Q^2+\sin^2(K_1D)/\sin^2(NK_1D)}, \tag{35}$$

where

$$Q^2=4q_\theta^4[\cos(k_yd_1)-q_\theta^2\sin(k_yd_1)]^2, \tag{36}$$

and the dispersion dependence K_1 (k_y) is determined by Eq. (24). Correspondingly, the transmission rate $|T|^2=1-|R|^2$ may be written as

$$|T|^2=\frac{1}{1+Q^2\sin^2(NK_1D)/\sin^2(K_1D)}. \tag{37}$$

Note that the ratio $\sin(K_1D)/\sin(NK_1D)$ may be presented as finite power series in $\sin^2(K_1D)$. Hence, by appeal to Eq. (24), the reflection coefficient R Eq. (34) for any given N may, in principle, be cast into the form of algebraic rational function of $\cos(k_yd_{1,2})$ and $\sin(k_yd_{1,2})$, with complex-valued coefficients including parameters N and q_θ^2.

IV. ANALYSIS OF THE DIFFRACTION SPECTRUM

A. Equidistant superlattice

First, we consider the superlattice constituted by domains of the same width d, so that the period is $D=2d$. Accordingly, the dispersion relation (24) simplifies to the form

$$\cos(K_1D)=2[\cos(k_yd)-q_\theta^2\sin(k_yd)]^2-1, \tag{38}$$

therefore, $Q^2=4q_\theta^4\cos^2(\frac{1}{2}K_1D)$, and

$$|R|^2=\frac{q_\theta^4}{q_\theta^4+\sin^2(\frac{1}{2}K_1D)/\sin^2(NK_1D)}. \tag{39}$$

The spectrum of the reflection-rate amplitude $|R(k_yD)|^2$, described by Eq. (39), consists of periodically repeated principal Bragg peaks and racks of secondary maximums alternating with zeros of reflection (Fig. 2). Its appropriate inversion gives the transmission spectrum $|T(k_yD)|^2$. Comparing the spectrum $|R|^2$, which is obtained from Eq. (39), with the exact numerical calculation, based on the definition (7) [i.e., with no appeal to Eq. (22)], shows satisfactory conformity already for the first Bragg peak and perfect confluence in the higher-frequency part of the spectrum (inset in Fig. 2). Inspection of Eq. (39) in conjunction with Eq. (38) allows for analytical description of the features of the spectral dependence of $|R(k_yD)|^2$.

By Eq. (39), the *SH* wave travels through the domain superlattice without reflection ($R=0$, $|T|=1$) at

$$(K_1D)_0^{(n)}=\frac{\pi n}{N}, \tag{40}$$

where n is not divisible by $2N$. At

$$(K_1D)_{\text{sm}}^{(n)}=\frac{\pi}{2N}(1+2n), \tag{41}$$

the value of the reflection-coefficient amplitude attains secondary maximums

$$|R|_{\text{sm}}^2=\frac{q_\theta^4}{q_\theta^4+\sin^2[\pi(1+2n)/4N]}. \tag{42}$$

Substituting Eqs. (40) and (41) into Eq. (38) reveals the location of the reflection zeros and secondary maximums in the spectrum. There are $2N-1$ reflection zeros alternating with $2N-2$ secondary maximums between each two neighboring principal peaks in the spectrum $|R(k_yD)|^2$.

The Bragg-type resonances, associated with the synchronism of reflections from the neighboring interfaces of $+/-$ and $-/+$ types, occur in the spectral ranges termed stop bands. According to Eq. (39), they are bounded by the condition

$$K_1D=2\pi l \quad (l=1,2,\ldots). \tag{43}$$

Hence, by virtue of Eq. (38), the edges of the lth stop band are determined as

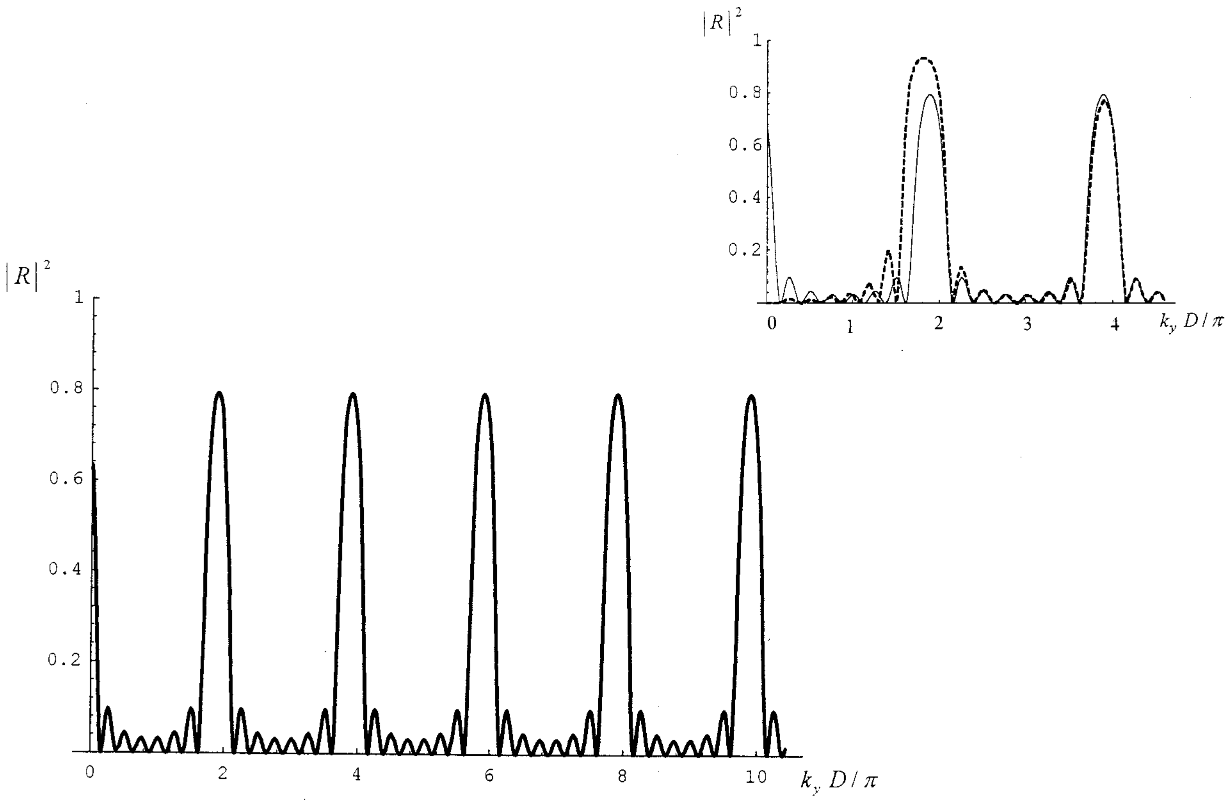

FIG. 2. Reflection rate $|R(k_yD)|^2$ for an equidistant superlattice $D=2d$ ($N=4$, $\theta=30°$, the value $q^2=0.31$ is taken for $BaTiO_3$ from Ref. 22). Inset shows the comparison with the exact calculation of $|R|^2$ (dashed line) via the definition (7).

$$(k_yD)_1=2\pi l-4\arctan(q_\theta^2),\quad (k_yD)_2=2\pi l, \tag{44}$$

so that its width in units k_yD is

$$\Delta_{\mathrm{band}}=4\arctan(q_\theta^2). \tag{45}$$

Using Eqs. (35), (43), at the edges of the stop bands,

$$|R|_{\mathrm{ed}}^2=1-\frac{1}{1+16q_\theta^4N^2}. \tag{46}$$

Inside the stop bands, the Bloch wave number K_1 takes complex values $K_1=2\pi l/D+iK_1'$. At the center of the lth stop band

$$(k_yD)_c=2\pi l-2\arctan(q_\theta^2) \tag{47}$$

the value $K_1'D$ reaches its maximum $(K_1'D)_{\max}\equiv\delta$, and hence the amplitude of the reflection coefficient attains its principal maximum value,

$$|R|_{\max}^2=\tanh^2(N\delta). \tag{48}$$

Inserting Eq. (47) and $K_1D=2\pi l+i\delta$ into Eq. (38) yields

$$\cosh\delta=1+2q_\theta^4. \tag{49}$$

Note that, by Eqs. (38), (49), the extremal values of the eigenvalues $\lambda_{1,2}=\exp(\pm iK_1D)$, taken in the center of a stop band, are $\lambda_{1,2}=1\pm2q_\theta^2\sqrt{1+q_\theta^2}+q_\theta^4$. Hence, they satisfy the inequality (28), which implies $\exp(k_xd)\sim\exp(\pi l\tan\theta)\gg q^2\tan\theta$. Defining the width $\Delta_{\max}$ of the principal peaks as the spectral distance (in units k_yD) between two zeros bordering the peak, we infer from Eqs. (40), (38) that

$$\Delta_{\max}=4\arccos\left(\frac{1}{\sqrt{1+q_\theta^4}}\cos\frac{\pi}{2N}\right). \tag{50}$$

It is seen that once the number of domains in the superlattice is large enough to fulfill $\pi/2N\ll q_\theta^2$, the width of principal peaks tends to the width of stop bands: $\Delta_{\max}\approx\Delta_{\mathrm{band}}$.

Typical values $q^2\lesssim0.1$ provide the strong inequality $q_\theta^2=q^2\tan\theta\ll1$ for a fairly wide range of values of the incidence angle θ. By Eq. (49), the value $\delta\equiv(K_1'D)_{\max}$ may be approximated at $q_\theta^2\ll1$ as $\delta\approx2q_\theta^2$, so that the height of the principal maximums is $|R|_{\max}^2\approx\tanh^2(2q_\theta^2N)$. In view of Eq. (50), its width at $\pi/2N\gg q_\theta^2$ is $\Delta_{\max}\approx2\pi/N$, while at $\pi/2N\ll q_\theta^2$ the width $\Delta_{\max}$ tends to $\Delta_{\mathrm{band}}\approx4q_\theta^2$. Relation (38) at $q_\theta^2\ll1$ and $|k_yD-2\pi l|\gg4q_\theta^2$ (i.e., remotely from stop bands) reduces to the form $k_yD\approx K_1D-2q_\theta^2$. It shows, with due regard for Eqs. (41), (42), (36), that the magnitude of secondary maximums $|R|_{\mathrm{sm}}$ is of the order of q_θ^2, and their width tends to half of the width of main peaks: $\Delta_{\mathrm{sm}}\approx\pi/N$. It is seen that a small value of the parameter q_θ^2 provides sharp selectivity of the spectrum.

Consider the case of incidence close to a grazing one ($\cos\theta\ll1$), which sets the inverse limiting inequality $q_\theta^2\gg1$. By virtue of Eqs. (45) and (50), $\Delta_{\mathrm{band}}\approx2\pi-4q_\theta^{-2}$, $\Delta_{\max}\approx2\pi-4q_\theta^{-2}\cos(\pi/2N)$, i.e., the principal peaks broaden and tend to the steplike shape, whereas the secondary maximums contract and steeply increase in height: $|R|_{\mathrm{sm}}^2\approx1$

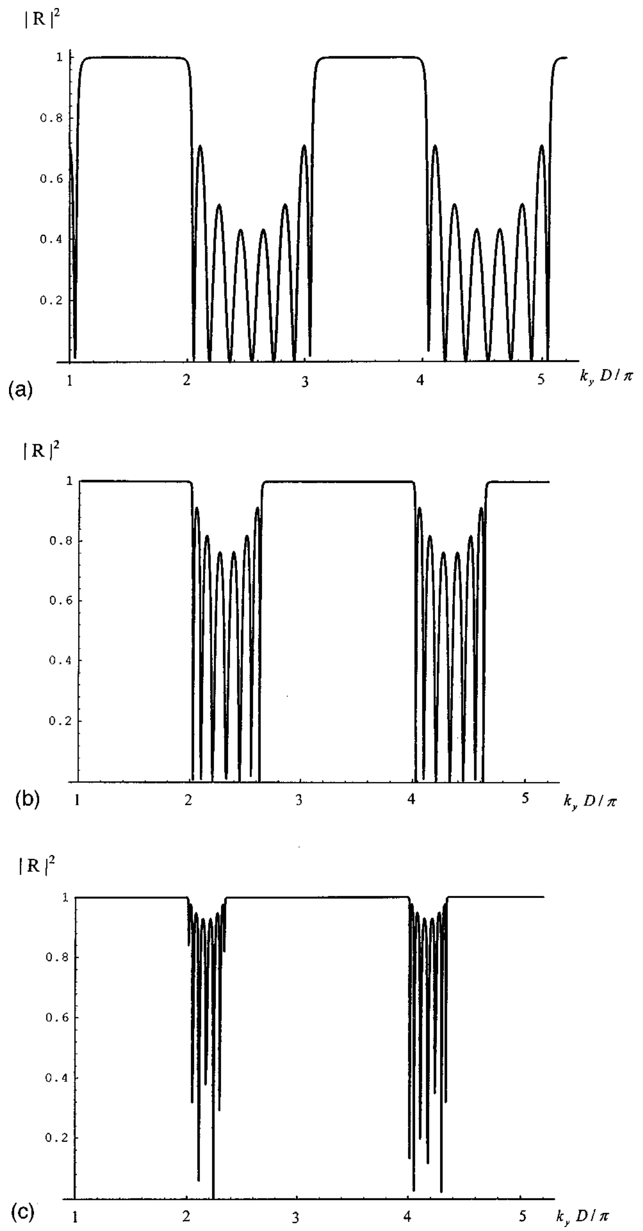

FIG. 3. Evolution of the reflection spectrum at the angle of incidence becoming close to a grazing one ($D=2d$, $N=4$, $q^2=0.31$). (a) $\theta=70°$; (b) $\theta=80°$; (c) $\theta=85°$.

$-q_\theta^{-4}\sin^2[\pi(1+2n)/4N]$ (Fig. 3). Simultaneously, the attainable range of the variable k_yD is shrinking. The exact grazing incidence under condition (22) entails the Maerfeld-Tournois evanescent wave[21] at the front interface.

B. Nonequidistant superlattice

In case of the nonequidistant superlattice ($d_1\neq d_2$), the stop bands of the *SH*-wave reflection spectrum $|R(k_yD)|^2$ Eq. (35) are defined by the relation

$$K_1D=\pi l \quad (l=1,2,\ldots). \tag{51}$$

This is different from condition (43) for the equidistant superlattice, in which case $K_1D=\pi(2l+1)$ equal to the odd number of π's brings about $R=0$ due to the antisynchronism of reflections from neighboring interfaces. Another basic feature, characterizing the nonequidistant superlattice, is that the Bragg maximums in the reflection and transmission spectra exhibit a certain modulation (see Refs. 4, 7, 11, 12, 18). This modulation, which may be observed at passing from Fig. 4(a) to Figs. 4(b) and 4(c), is governed by the relation between the widths d_1,d_2 of domains constituting a unit cell.

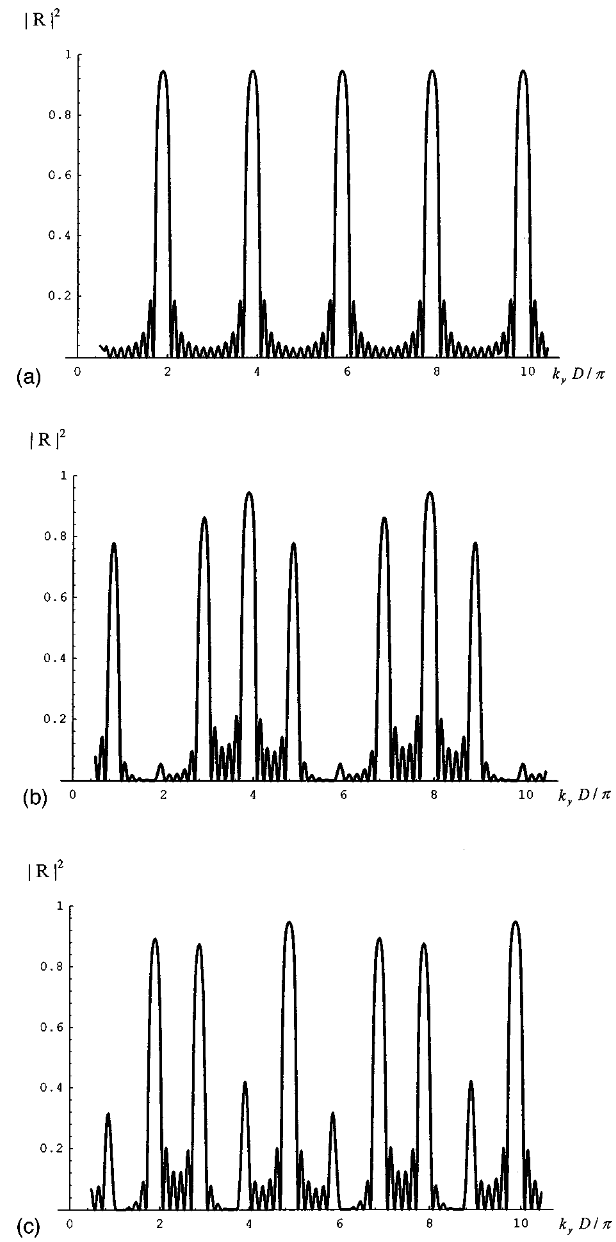

FIG. 4. Patterns of the reflection spectrum for different relations between widths d_1, d_2 of domains in a unit cell ($N=6$, $\theta=30°$, $q^2=0.31$). (a) $d_1/D=1/2$ (equidistant superlattice); (b) $d_1/D=2/5$ (the period of modulation of the Bragg peaks is $T=5$), (c) $d_1/D=1/4$ [the Bragg peaks of the orders $l=2+4m$ ($m=0,1,\ldots$) satisfy the extinction rule].

Inserting Eq. (51) into Eq. (24) and assuming $q_\theta^2\ll 1$ yields concise relations for the spectral positions of the edges of the lth stop band:

$$(k_yD)_1=\pi l-2q_\theta^2(1+|\cos[\pi l(d_1/D)]|),$$

$$(k_yD)_2=\pi l-2q_\theta^2(1-|\cos[\pi l(d_1/D)]|). \tag{52}$$

Taking the center of the lth stop band $k_yD=\pi l-2q_\theta^2$ gives $K_1D=\pi l+i\delta_l$, in which δ_l turns out to be the stop-band halfwidth (in units k_yD):

$$\delta_l=\frac{1}{2}\Delta_{\text{band}}=2q_\theta^2\left|\cos\left(\pi l\frac{d_1}{D}\right)\right|. \tag{53}$$

Under the condition $q_\theta^2\ll 1$, the reflection-rate amplitude at the edges of the lth stop band is

$$|R|_{\text{ed}}^2=1-\frac{1}{1+16N^2q_\theta^4\cos^2[\pi l(d_1/D)]}, \tag{54}$$

and its principal maximum value at the stop-band center follows in the form

$$|R|_{\max}^2=\tanh^2\left[2q_\theta^2N\left|\cos\left(\pi l\frac{d_1}{D}\right)\right|\right]. \tag{55}$$

Manipulating Eq. (24) gives the width between two zeros bordering the principal maximum as $\Delta_{\max}\approx 2\pi/N$ at $\delta_l\ll\pi/N$, and $\Delta_{\max}\approx\Delta_{\text{band}}$ at $\delta_l\gg\pi/N$.

Equations (52)–(55) reveal that the modulation of the Bragg peaks of $|R|$ is periodical, provided that the ratio of d_1 and $D=d_1+d_2$ is a rational fraction: $d_1/D=s/T$ (s, T are integers and T is not divisible by s). Then, each lth peak is repeated by the $(l+mT)$th ones $(m=1,2,\dots)$, see Fig. 4(b). Moreover, if the numerator s is odd and the denominator T is even, then the Bragg peaks with the numbers, satisfying the extinction rule

$$l=\frac{T}{2}+mT \quad (m=0,1,2,\dots), \tag{56}$$

are suppressed [Fig. 4(c)]. This is similar to the results, obtained for the piezocrystalline superlattice with cladding interfaces.[12,16]

V. SUMMARY

The Bragg-diffraction phenomenon arising at an oblique propagation of *SH* wave has been studied in the antiphase superlattice, which describes a system of 180° ferroelectric domains or a stack of piezoelectric layers with antiparallel orientation. The electromechanical coupling stipulates excitation of interface modes, so that the diffraction involves four modes in total and is described by the 4×4 propagator matrix **W**. Given that the wavelength is markedly less than the width of domains, which is the condition underlying diffraction resonances, the two interface modes are characterized by large coefficients of exponential decrease/increase. This feature leads to the exponentially strong inequalities between corresponding eigenvalues of **W**. Taking note of them and utilizing appropriate matrix algebra has provided the explicit analytical description of the reflection and transmission spectra. In turn, it allowed for direct inspection of the resonant features of diffraction, controllable by the parameter of electromechanical coupling, frequency, angle of incidence, number of domains, and the pairwise ordering of widths of domains in a unit cell.

It is noteworthy that the developed algebraic method, which essentially employs the presence of interface modes, may also be applied to the study of reflection transmission of a sagittal wave in elastic multilayers at such angles of incidence, when the other sagittal-wave branch yields interface modes.

ACKNOWLEDGMENTS

The authors are grateful to Dr. I. Jefferson for useful comments. This work was supported by the Russian Foundation for Basic Research under Grant No. 97-02-16338.

*Author to whom correspondence should be addressed. Electronic address: ashuv@mechan.incr.msk.su

[1] B. Djafari-Rouhani, L. Dobrzynski, O. Hardouin Dupare, R. E. Camley, and A. A. Maradudin, Phys. Rev. B **28**, 1711 (1983).
[2] A. Nougaoui and B. Djafari-Rouhani, Surf. Sci. **185**, 125 (1987); **185**, 154 (1987).
[3] L. Fernández, V. R. Velasco, and F. Garcia-Moliner, Surf. Sci. **188**, 140 (1987).
[4] S. Tamura and J. P. Wolfe, Phys. Rev. B **35**, 2528 (1987).
[5] L. P. Zinchuk, A. N. Podlipinets, and N. A. Shul'ga, Sov. Appl. Mech. **24**, 245 (1988).
[6] V. I. Alshits, V. V. Antipov, S. I. Chizhikov, A. N. Darinskii, N. G. Sorokin, and A. L. Shuvalov, Ferroelectrics **96**, 91 (1989).
[7] S. Tamura, Phys. Rev. B **39**, 1261 (1989).
[8] Li Xingjiao, Li Yibing, Li Shaoping, L. E. Cross, and R. E. Newnham, J. Phys.: Condens. Matter **2**, 9577 (1990).
[9] V. G. Mozhaev, G. N. Morozova, and O. Yu. Serdobol'skaya, Sov. Phys. Solid State **32**, 1872 (1990).
[10] A. H. Nayfeh, J. Acoust. Soc. Am. **89**, 1521 (1991).
[11] Y. Y. Zhu and N. B. Ming, J. Appl. Phys. **72**, 904 (1992).
[12] V. I. Alshits and A. L. Shuvalov, Phys. Lett. A **177**, 253 (1993); J. Appl. Phys. **77**, 2659 (1995).
[13] Y. Y. Zhu, N. B. Ming, and A. L. Shuvalov, J. Phys. B **5**, 1139 (1993).
[14] E. H. El Boudouti, B. Djafari-Rouhani, and A. Nougaoui, Phys. Rev. B **51**, 13 801 (1995).
[15] D. V. Roshchupkin, S. V. Tkachev, R. Ticoulou, M. Brunel, and A. Sergeev, Ferroelectr. Lett. Sect. **19**, 139 (1995).
[16] V. I. Alshits, A. S. Gorkunova, and A. L. Shuvalov, Sov. Phys. JETP **83**, 509 (1996).
[17] E. L. Shenderov, J. Acoust. Soc. Am. **101**, 1239 (1997).
[18] H. Kato, J. Acoust. Soc. Am. **101**, 1380 (1997).
[19] F. R. Gantmakher, *The Theory of Matrices* (Chelsea, New York, 1960).
[20] A. M. B. Braga and G. Herrmann, J. Acoust. Soc. Am. **91**, 1211 (1992).
[21] C. Marfeld and P. Tournois, Appl. Phys. Lett. **19**, 117 (1971).
[22] A. V. Turik, Fiz. Tverd. Tela (Leningrad) **12**, 892 (1970).